An Investigation of force components in orthogonal cutting of medical grade cobalt chromium alloy (ASTM F1537)

S.Baron, *University College Dublin.* **E.Ahearne,** *University College Dublin.*

An aging population, increased physical activity and obesity, are identified as life style changes contributing to growth in the use of in-vivo prosthetics for total hip and knee arthroplasty. Cobalt chromium alloys, due to mechanical properties and excellent biocompatibility, uniquely qualify as a class of materials that meet the stringent functional requirements for these devices. To cost effectively assure the required dimensional and geometric tolerances, manufacturers invariably rely on high precision machining. However, a comprehensive literature review has shown that there has been limited research into mechanical cutting of these materials.
This paper delineates the physical and mechanical properties that determine the machinability of a material, and compares medical grade cobalt chromium alloy ASTM F1537 with titanium alloy, Ti-6Al-4V ASTM F136. The results of a full factorial orthogonal cutting experiment are reported where cutting and thrust force components were measured over a range of cutting speeds (V_c) and levels of undeformed chip thickness (h_m). It was found that the forces generated in cutting of ASTM F1537 are significantly higher than for ASTM F136, depending primarily on undeformed chip thickness, but with some influence of the cutting speed. The effect of chip segmentation on component force variations is also reported.
Keywords: Cobalt Chromium Alloys, Orthogonal Cutting, Forces in Cutting

Introduction:

Medical grade cobalt chromium alloys (CoCr) are a range of materials commonly used for components of implantable medical devices. This is due to a range of required physical and mechanical properties but notably, excellent biocompatibility and high wear resistance. Typical applications include: high precision components for total knee arthoplasty (Figure 1) and total hip replacement.

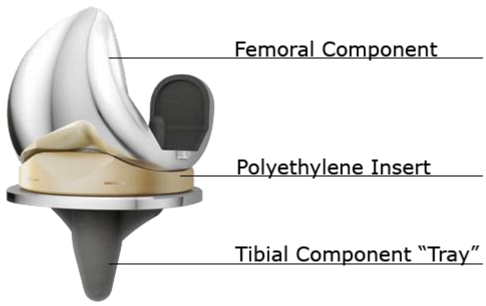

Figure 1: Main components for total knee arthoplasty

The objective of the research now reported is to determine the effect of the critical control parameters, cutting speed (V_c) and the undeformed chip thickness (h_m), on the main force components in orthogonal cutting of medical grade CoCr ASTM F1537, comparing it directly with medical grade Titanium alloy, Ti-6Al-4V ASTM F136. A description of CoCr alloys is first presented in terms of microstructure, physical and mechanical properties, and two CoCr alloys are compared in that regard with the Titanium alloy, assessing the machinability of the materials from this comparison. A full factorial orthogonal cutting experiment is then described and results presented to enable comparison of measured force components for CoCr ASTM F1537 and Ti-6Av-4V ASTM F136. The results are analysed in terms of the main effects but also in terms of the superposed high frequency cyclical force due to chip segmentation. The

discussion that follows summarises the findings and advances some hypotheses. The objectives and plans for future research into the fundamental mechanisms and models in cutting are also outlined.

Literature Review:

CoCr alloys, first synthesized by Haynes in 1907, are characterised by a high strength and low chemical reactivity [1]. Alloying with Molybdenum (Mo) or Tungsten (W) significantly increases the alloy's strength. The primary cobalt metal will form a metastable HCP ε phase, even at room temperature [2]. FCC structure dominates in CoCrMo alloys which are characterised as high strength with high strain hardening rates and the ability to absorb stresses by FCC to HCP transformation [3, 4]. CoCr alloys exhibit a two phase dendritic solidification process. Dendritic regions are nobler, rich in cobalt ($\gamma - phase$) and have a FCC structure. Interdendritic regions are the less noble phase with a HCP structure [5]. An equilibrium diagram, developed for the CoCr binary, is shown in figure 2 indicating the microstructural changes under thermodynamic equilibrium conditions [6].

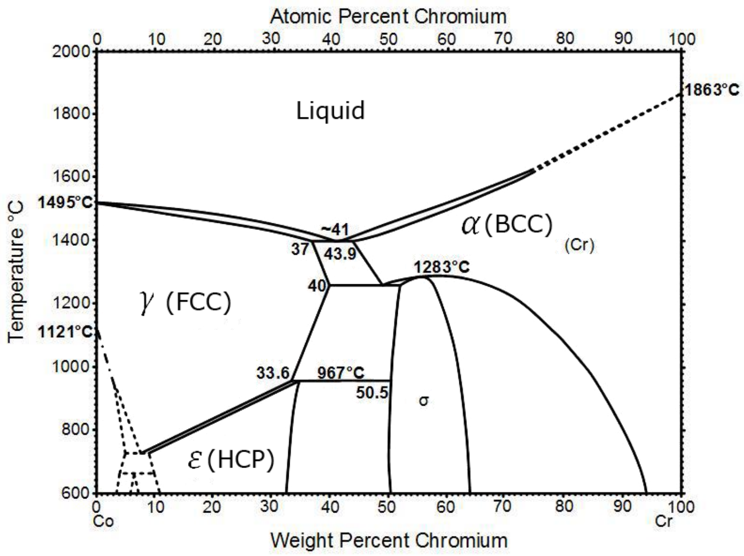

Figure 2: Phase diagram of binary CoCr alloy [7].

Increasing the chromium content improves corrosion resistance but also interacts with carbon to form hard carbides which improves the alloys strength, hardness and corrosion resistance [4]. These carbides are found to:
(a) Disperse in the matrix, increasing the strength of the alloy, and
(b) Precipitate at the grain boundaries supressing gross sliding and dislocation migration.

Alloy Standard Specification:	Units	CoCr ASTM F1537	CoCr ASTM F75*	Ti-6Al-4V ASTM F136
Tensile Strength	**[MPa]**	1403	920	940
0.2% Proof Stress	**[MPa]**	928	527	870
Elongation	**[%]**	29	16.5	16
Young's Modulus	**[GPa]**	283	216	114
Hardness	**[HRC]**	40	32.8	31
Thermal Conductivity (K)	**[$W.m^{-1}.K^{-1}$]**	14.8	13	7.2
Specific Heat Capacity (Cp)	**[$J.Kg^{-1}.K^{-1}$]**	452	450	560
Density (ρ)	**[$Kg.m^{-3}$]**	8,250	8,300	4,420
Thermal Diffusivity	**[$m^2.s^{-1}$]**	3.73E-06	3.00E-06	2.91E-06
K* Cp* ρ		13.91	11.21	7.20

Table 1: Summary of mechanical properties of biomedical CoCr ASTM F1537, F75 and Ti ASTM F136 alloys. ASTM F75 -Hot Isostatic Pressing was performed.*

Alloying with molybdenum creates new M_7C_3, $M_{23}C_6$ and M_6C carbides, further improving the mechanical properties of the alloy [4]. Formation, dispersion and precipitation of these hard carbides are the primary strengthening mechanisms of the CoCr alloys [8]. The mechanical properties of ASTM F1537, ASTM F75 and ASTM F136 are summarised in table 1.
Further improvement of the mechanical properties of cast the CoCrMo alloy is achieved by a careful post casting treatment. Solution treatment allows for partial or complete dissolution of precipitates while the hot isostatic (HIP) pressing causes collapse of internal pores within the material bulk, enhancing its ductility [2]. The HIP process on ASTM F75 alloy can increase tensile strength by up to 40% [2, 4].

According to Shaw [9], the machinability of a material is based on (1) Tool life (2) Surface finish and (3) Power required to cut. The machinability is in turn dependent on physical and mechanical properties of the material; properties that vary under the extreme stresses, strains, strain rates and temperatures in cutting. The key properties include:

(a) The flow stress (σ_y) which is a function of strain, strain rate, and temperature; often characterised by the ubiquitous Johnson-Cook equation.
(b) The thermal diffusivity which determines how effectively a given material can dissipate generated heat, and thus affects the temperature in the shear zones and on the tool surfaces. It is related to thermal conductivity, density and specific heat capacity.
(c) Friction at tool-work piece interface which depends on the nature of the friction mechanisms (adhesion, abrasion, physio-chemical reactions etc.) and therefore more detailed tool and material properties as well as process parameters related to coolant application strategy [9].

As shown in table 1, ASTM F1537 has a higher tensile strength, hardness and elongation than ASTM F75 and ASTM F136 where F75 is within 10% of F136 for all these properties. Table 1 also shows the product (K* Cp* ρ) which, based on a simplified “moving heat source” model in [9], is inversely related to the maximum temperature on the idealised “tool-work interface”. The value of this product is lowest for Titanium which is a baseline material in terms of relatively high temperatures during cutting. The consequent high rate of tool wear variation with cutting speed, classifies Titanium as a “difficult-to-cut” material. However, the values of this product for ASTM F1537 and F75, at less than double the value for Titanium, should be compared with 1020 steel and 75ST aluminium at about 4 and 5 tomes respectively. Of course, the properties in table 1 are compared under at room temperature in the absence of constitutive equations relating material properties to state variables. Thus, the machinability is a complex function of material, tool and process parameters but the materials can be compared by an experimental approach as now follows.

Experimental Method:

In order to examine the forces in cutting of the ASTM F1537 CoCrMo for comparison with Ti-6Al-4V F136 a full factorial, orthogonal cutting experiment was performed. The cutting forec, F_c, and thrust forces, F_t, were recorded at discrete levels of the experimental parameters:

1) Cutting speed- V_c.
2) Undeformed chip thickness- h_m.

The tests were carried out on the HAAS TL2 CNC lathe. Forces were recorded using piezoelectric dynamometer system which comprises: a Kistler type 9272 dynamometer, a Kistler 50019 charge amplifier, a NI DAQ 6024E data acquisition card and LabView software. In order to measure the force components in the required ranges, and with the required frequency response, a tool clamping/fixing assembly integrated in a Kistler dynamometer was designed as shown in Figure 3. The sampling rate was set to 1 kHz. The CoCr alloy, ASTM F1537, was tested for all independent parameter levels in the full factorial experiment while ASTM F136 Ti-6Al-4V was tested only at V_c= 23 & 70 m/min and h_m= 15 & 30μm. The experimental parameters were selected based on the literature review for Titanium [11-13] and preliminary cutting trials conducted as per cutting tool supplier recommendations [14]. The computed details on the cutting conditions are presented in

Table 2. Sample of the chips formed in each test was collected, mounted in epoxy resin, ground and polished. A microscopic examination measured the median segment length (L_c), the segment height and maximum chip thickness (L_s) [11, 15], as shown on Figure 6. The median of the cutting force components, under steady state cutting conditions, was estimated from a minimum of 1000 data points.

CUTTING CONDITIONS:					
Test Parameter	Units:	Value:			
Cutting Speed:	**[l.min⁻¹]**	23	36	48	70
Undeformed Chip Thickness:	**[µm]**		15	30	45
Disc Width:	**[mm]**	3			
Rake Angle:	**[°]**	0			
Relief Angle:	**[°]**	7			
Cutting Edge Radius:	**[µm]**	14			
Insert Type:	**N/A**	SCMW 120408 H13A			
Coolant Type::	**N/A**	FUSCH ECOCOOL ULTRALIFE A			
Coolant Flow:	**[l.min⁻¹]**	2.5			
Coolant Concentration:	**[%]**	8.50			

Table 2: The experimental cutting conditions.

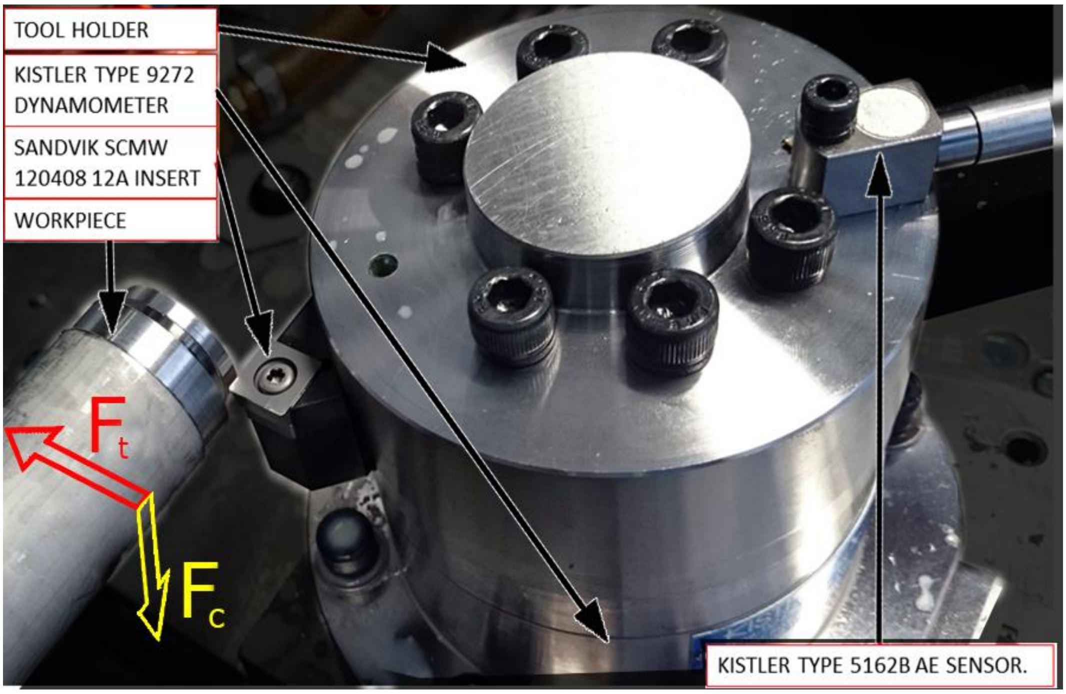

Figure 3: The experimental setup displaying the configuration of the orthogonal turning test.

Results and Discussion:

The median values of F_t and F_c for the CoCr alloy are presented in table 3, while median values of F_t and F_c for Ti-6Al-4V are presented in Table 5. The results for both alloys are plotted and compared in Figures 4 and 5. It is evident that the median values of the cutting and thrust force components increase with the undeformed chip thickness for both CoCr alloy and Ti-6Al-4V. The median value of the vertical force component (F_c) was generally higher than the horizontal component (F_t), although with an exception at high undeformed chip thickness and low cutting speed for CoCrMo and Ti-6Al-4V; this is highlighted in Table 3 and Table 4.

F_t [N]		h_m [μm] 15	30	45	F_c [N]		h_m [μm] 15	30	45
V_c [m/min]	25	437.5	502.5	684.8	V_c [m/min]	25	473.2	462.9	539.1
	36	373.5	523.7	710.0		36	482.0	560.3	579.6
	48	379.4	538.4	639.5		48	512.0	578.0	603.3
	70	349.4	627.0	892.8		70	445.4	696.8	969.0

Table 3: The median values of force reading in F_t and F_c for ASTM F1537 CoCrMo.

F_t St.D [%]		hm [μm] 15	30	45	F_c St.D [%]		hm [μm] 15	30	45
Vc [m/min]	25	9.0	20.5	85.5	Vc [m/min]	25	19	28.9	42.0
	36	5.8	9.0	18.0		36	7.5	12.8	19.6
	48	4.2	5.4	18.5		48	2.6	9.3	16.3
	70	4.9	10.8	8.4		70	4.6	12.0	11.2

Table 4: The standard deviation of the mean of F_t and F_c for ASTM F1547 CoCrMo

Ti-6Al-4V								
CONDITIONS:	V_c=25 h_m=15		V_c=25 h_m=30		V_c=70 h_m=15		V_c=70 h_m=30	
CHANNEL:	F_c	F_t	F_c	F_t	F_c	F_t	F_c	F_t
Force Reading:	209	231	325	257	212	230	346	273
St.Dev	7.72	8.36	15.60	13.17	12.04	11.80	29.27	25.50

Table 5: The median values of Force components (F_t & F_c) standard deviation for Ti-6Al-4V.

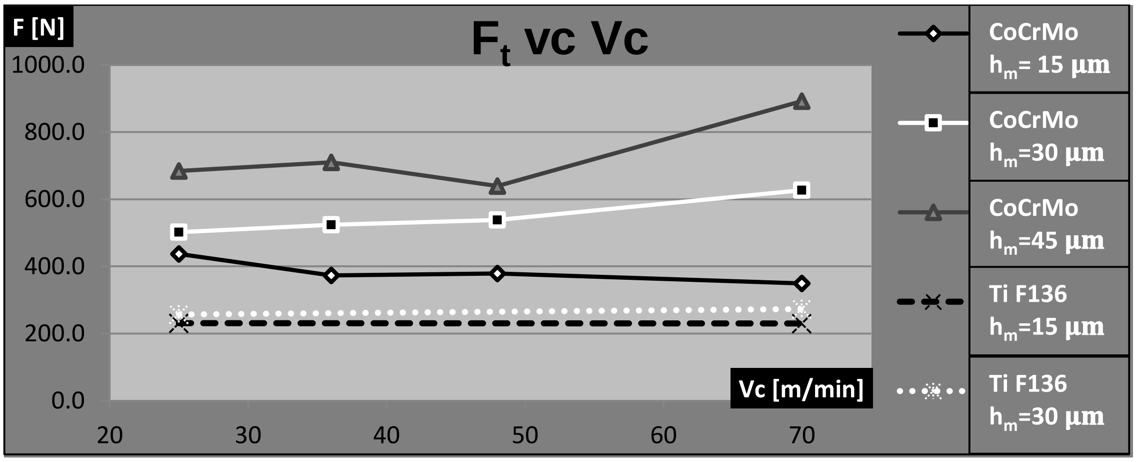

Figure 4: The plot of F_t as a function of V_c for ASTM F1536 & ASTM F136.

F_t and F_c appear to be relatively independent of V_c, with the exception for CoCrMo at V_c=70m/min. The median values of both force components were found to increase at V_c=70 m/min and h_m= 30 μm & 45 μm. Simultaneously the standard deviation of these median values was relatively low (≤ 12%)- See Table 4. Examination of the chip cross section has a shown that the CoCr alloy formed the characteristic, shear localised (saw tooth) chip under all tested conditions. The segment length (L_c) and segmentation ratio (h_s/h_c), were found to depend on the cutting conditions.

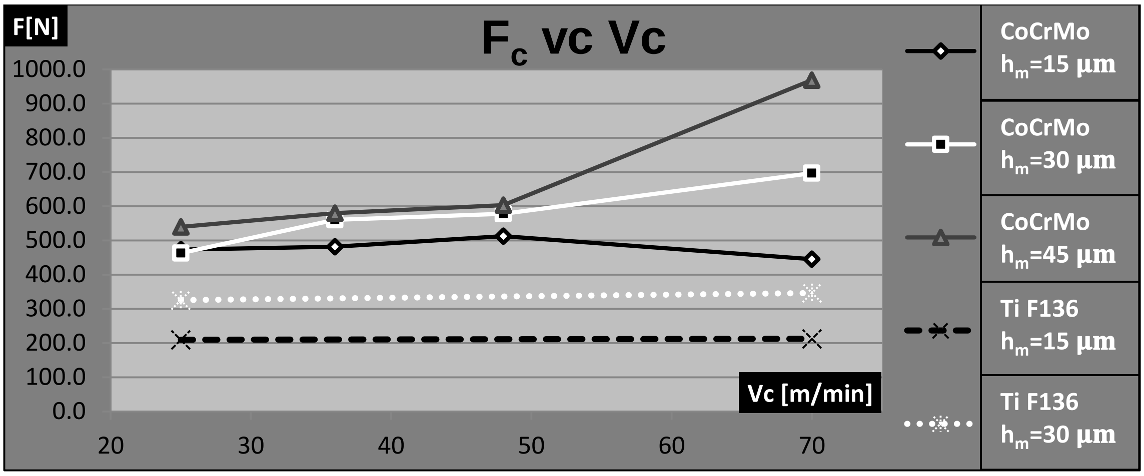

Figure 5: The plot of F_c as a function of V_c for ASTM F1536 & ASTM F136.

The chip segmentation ratio was higher for low V_c and was found to be relatively independent of h_m. This is reflected in a higher standard deviation and may explain why the median of F_t is greater than F_c for these conditions.

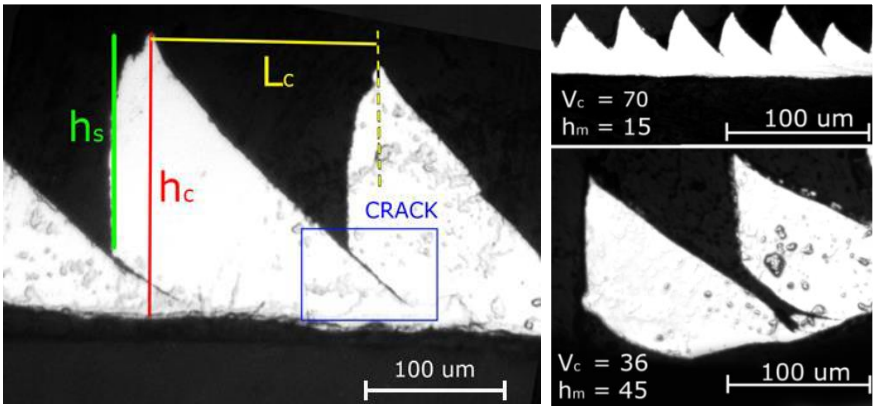

Figure 6: ASTM F1537 CoCrMo Chip morphology.

Conclusions:

Based on this experimental investigation into the cutting forces in the orthogonal turning of ASTM F1537 it may be concluded that:

1) The cutting forces in orthogonal cutting of ASTM F1537 CoCr alloy are notably higher than in case of ASTM F136 Ti-6Al-4V.
2) The cutting forces in orthogonal cutting of ASTM F1537 and ASTM F136 were found to primarily depend on the undeformed chip thickness.
3) The cutting forces in orthogonal cutting of ASTM F1537 CoCr alloy, while remaining relatively independent of cutting speed (up to 48 m/min), were found to notably increase at V_c=70 m/min.
4) In orthogonal cutting of the CoCr alloy, a segmented (saw tooth) chip formation was observed where its geometry was found to significantly depend on V_c and h_m.

Furthermore it was observed that the chip segmentation was primarily dependent on V_c as previously shown by the authors in [15]. It was also observed that, for CoCr alloy at V_c of 25-48 m/min, and h_m of 30 and 45 um, the mean of F_t was higher than F_c. Under those cutting conditions a high fluctuation in the force reading was noted which is reflected by the high standard deviation.
Examination of the chip morphology may suggest that the segmented chip was formed by a crack initiation mechanism as described in [16]. This crack originates at the free surface and

propagates towards the tool tip as shown in Figure 6 (left). The chip segment height h_s decreases as the V_c increases. This is reflected in the chip segmentation ratio which was observed to correlate with the standard deviation of the force reading (Figure 6 and Table 4).

Acknowledgements:

We would like to thank DePuy Synthes and Enterprise Ireland for funding this research through the Innovation Partnership (IP) programme. The IP programme is co-funded by the European Union through the European Regional Development Fund 2014-2020.

References:

1. Al Jabbari, Y.S., *Physico-mechanical properties and prosthodontic applications of Co-Cr dental alloys: a review of the literature.* The journal of advanced prosthodontics, 2014. **6**(2): p. 138-145.
2. R.Kaiser, *Study of the Effect of Casting Variables and Heat Treatment Procedure on the Microstructure and mechanical Properties of Co-Cr-Mo Biomedical Alloy*, in *School of Mechanical and Materials Engineering*. 2013, University College Dublin: Dublin.
3. Bedolla-Gil, Y. and M. Hernandez-Rodriguez, *Tribological behavior of a heat-treated cobalt-based alloy.* Journal of materials engineering and performance, 2013. **22**(2): p. 541-547.
4. Sikkenga, C. and C.A. Castings, *Casting, vol. 15.* ASM Handbook, ASM International, 2008: p. 1114-1118.
5. Montero-Ocampo, C., R. Juarez, and A.S. Rodriguez, *Effect of fcc-hcp phase transformation produced by isothermal aging on the corrosion resistance of a Co-27Cr-5Mo-0.05C alloy.* Metallurgical and Materials Transactions A, 2002. **33**(7): p. 2229-2235.
6. Matković, T., P. Matković, and J. Malina, *Effects of Ni and Mo on the microstructure and some other properties of Co–Cr dental alloys.* Journal of Alloys and Compounds, 2004. **366**(1–2): p. 293-297.
7. Ishida, K. and T. Nishizawa, *The Co-Cr (cobalt-chromium) system.* Bulletin of Alloy Phase Diagrams, 1990. **11**(4): p. 357-370.
8. Ramírez-Vidaurri, L., et al., *Cooling rate and carbon content effect on the fraction of secondary phases precipitate in as-cast microstructure of ASTM F75 alloy.* journal of materials processing technology, 2009. **209**(4): p. 1681-1687.
9. Shaw, M.C., *Metal cutting principles*. Vol. 2. 2005: Oxford university press New York.
10. Varano, R., et al., *The effect of microstructure on the wear of cobalt-based alloys used in metal-on-metal hip implants.* Proceedings of the Institution of Mechanical Engineers, Part H: Journal of Engineering in Medicine, 2006. **220**(2): p. 145-159.
11. Cotterell, M. and G. Byrne, *Characterisation of chip formation during orthogonal cutting of titanium alloy Ti–6Al–4V.* CIRP Journal of Manufacturing Science and Technology, 2008. **1**(2): p. 81-85.
12. Cotterell, M. and G. Byrne, *Dynamics of chip formation during orthogonal cutting of titanium alloy Ti–6Al–4V.* CIRP Annals - Manufacturing Technology, 2008. **57**(1): p. 93-96.
13. Ezugwu, E.O. and Z.M. Wang, *Titanium alloys and their machinability—a review.* journal of materials processing technology, 1997. **68**(3): p. 262-274.
14. Sandvik, *GENERAL TURNING*. 2015, Sandvik: www.coromat.sandvik.com.
15. Baron, S. and Ahearne, E., *Characterization of Chip Morphology in Orthogonal Cutting of Medical Grade Cobalt Chromium Alloy (ATM F1537)*, in *International Manufacturing Conference 32*. 2015: Queen's University Belfast.
16. Zhang, S., et al., *Saw-tooth chip formation and its effect on cutting force fluctuation in turning of Inconel 718.* International Journal of Precision Engineering and Manufacturing, 2013. **14**(6): p. 957-963.